IEEE Access
Multidisciplinary | Rapid Review | Open Access Journal

Received June 28, 2019, accepted July 15, 2019, date of publication July 29, 2019, date of current version August 13, 2019.

Digital Object Identifier 10.1109/ACCESS.2019.2931492

Electric Field Distribution Characteristics and Space Charge Motion Process in Transformer Oil Under Impulse Voltage

BO QI[1], (Member, IEEE), CHUNJIA GAO[2], HAO HAN[1], XIAOLIN ZHAO[2], QING YUAN[1], SHUQI ZHANG[2], AND CHENGRONG LI[1], (Senior Member, IEEE)

[1]State Key Laboratory of Alternate Electrical Power System with Renewable Energy Sources, North China Electric Power University, Beijing 102206, China
[2]China Electric Power Research Institute, Beijing 100192, China

Corresponding author: Bo Qi (lqicb@ncepu.edu.cn)

This work was supported in part by the Natural Science Foundation of Beijing Municipality under Grant 3172033, and in part by the National Key Research and Development Program of China under Grant 2017YFB0902704.

ABSTRACT The electric field and space charge dynamics characteristics in oil under impulse voltage are key factors to the transformer insulation design, which are mainly obtained through simulation, falling short of experimental verifications. Applying the Kerr electro-optic method, the present paper carried out an actual measurement for the electric field characteristics in transformer oil under impulse voltage and managed to obtain their correlations with an electrode material, voltage amplitude, and wave-front time, respectively. First, it was found that, under impulse voltage and in pure transformer oil, the aluminum electrode had the largest amount of charge injection, followed by stainless steel and then copper, which was attributed to the different work functions of metal elements in electrodes. Second, with the increase of voltage amplitude, the effect of the space charge on the intermediate electric field of the oil gap was first enhanced, then weakened, and eventually enhanced. Third, as the wave-front time was prolonged, the peak of electric field in transformer oil showed a downward trend. For instance, the peak value of the electric field was reduced by 17.6 % when the wave-front time was increased from 0.5 μs to 40.0 μs. The reason is that when the wave-front time is longer, the amount of injected charge grows larger and the weakening effect becomes stronger. Fourth, a charge dynamic motion model in transformer oil under impulse voltage was established to demonstrate its spatial-temporal effects on the electric field. Besides, this paper has clarified the source of the negative and positive charges in the transformer oil under impulse voltage by using the theories of field emission and field ionization. Moreover, the variation of electron mobility over-voltage amplitude, wave-front time, and spatial distribution was worked out to present the quantitative results of its motion process.

INDEX TERMS Electric field, distribution characteristics, charge motion process, electron mobility, transformer oil, impulse voltage.

I. INTRODUCTION

Transformer is one of the core apparatuses for electric energy conversion and transmission in power system [1]. The transformer oil, which has the advantages of well insulation performance and dielectric properties, is adopted as the main insulation dielectrics of transformer. At present, in the concerned of insulation design, the commercial simulation software is commonly utilized to calculate and analyze the electric field of insulation structure based on the principle of capacitive voltage division, and then a reasonable safety margin is taken as the additional guarantee [2]. Some certain literatures have reported that there could generate space/interface charge accumulation or migration under voltage applications, which could exert a non-negligible effect on the electric field, bringing out the challenges to the effectiveness of insulation design. It indicates that the existing simulation methods have certain limitations to meet the transformer insulation design requirements, and the effectiveness of which falls short of verification from actual measurement. The impulse voltage application is one of the operating conditions of transformers, and a number of cases have been reported about that many

The associate editor coordinating the review of this manuscript and approving it for publication was Kan Liu.

 This work is licensed under a Creative Commons Attribution 4.0 License. For more information, see http://creativecommons.org/licenses/by/4.0/

transformers had suffered from insulation damage due to lightning strike during field operation or routine test before delivery [3]. Thus, it is very necessary to carry out the actual measurement of the electric field characteristics in the transformer oil under the impulse voltage, explore the space charge motion process, and reveal its dynamic laws in transformer oil.

Scholars have already conducted a certain number of studies in relation to the characteristics of electric field and space charge in liquid dielectrics. As for the electric filed measurement approaches in liquid dielectrics, the Kerr electro-optic method has been proved as one of the most effective non-contact measuring methods. By photographing electro-optic interference patterns under impulse voltage, the electric field distribution characteristics in high Kerr-constant liquids such as nitrobenzene, purity water, and propylene carbonate in different electrode combinations and structures were obtained [4]–[6]. It was found that the copper electrodes bi-polarly injected positive and negative charges into anode and cathode respectively, the aluminum electrodes unipolarly injected negative charges only, and the stainless steel unipolarly injected positive charges alone. When the bipolar space charges were injected, the electric field distribution between electrodes could be improved more uniformly, and the breakdown strength of the liquid dielectric could also increase due to the shielding effect of space charges. On the contrary, the unipolar charge injection worsened the electric field distortion and also reduced the insulation properties of the liquid dielectric. Applying the theory of ion migration and introducing the equation of thermal diffusion, O'Sullivan modeled and analyzed the charge transfer process in liquid dielectric [7]. Drawing the finding from precious researches and based on the electric field measurement results in propylene carbonate, Sima et al established charge injection and migration model based on the theory of electric double layer [8]. Qi et al explored the polarity effect of the positive and negative charge accumulation at the oil-paper insulation interface through measuring the distribution of electric field under DC voltage, AC-DC combined voltage and polarity reversal voltage, and pointed out the limitations of the widely-used Resistive-Capacitive model (RC model) [9]–[11].

In summary, the existing researches make use of either high Kerr constant liquids for equivalent measurements, or experiment at low field-strength DC voltages. Few researches have been carried out on the characteristics of electric field and space charge motion process in transformer oil under impulse voltage.

Adopting the Kerr electro-optic method, the present paper established a measurement platform for electric field in transformer oil under impulse voltage, studied the electric field characteristics and its correlation with electrode material, voltage amplitude, wave-front time, and spatial location respectively, and clarified the charge motion process based on the measured characteristics. It is expected that the research findings could provide useful references for the insulation design of power transformers.

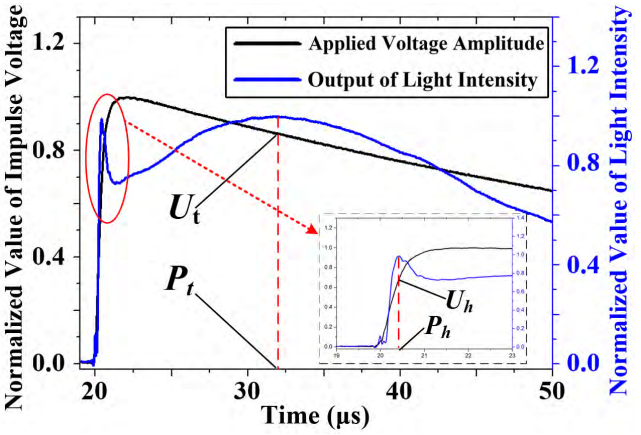

FIGURE 1. Normalized curves of applied impulse voltage and light intensity.

II. THE PRINCIPLE OF ELECTRIC FIELD MEASUREMENT

Under the impact of the electric field, the transformer oil exhibits the effect of birefringence. A phase difference θ occurs between the light intensity component which is perpendicular to the direction of the electric field and the light intensity component which is parallel to the direction of the electric field [9]–[11]. This phase difference is proportional to the Kerr constant of the liquid medium, the length of the electric field region, and the square of the electric field strength. Given the specific optical path, the output light intensity and the input light intensity bear such a relation to the applied electric field E is shown as follows [11].

$$\frac{I_o}{I_i} = \sin^2[\frac{\pi}{2}(\frac{E}{E_m})^2] \tag{1}$$

In equation (1), I_i denotes the input light intensity, I_o marks the output light intensity, and E_m represents the electric field strength when the light intensity reaches the first peak value, which is only related to the Kerr constant B of the oil and the length L of the measured electric field region, as shown in equation (2) [11].

$$E_m = \frac{1}{\sqrt{2BL}} \tag{2}$$

According to the actual situation of the measurement equipment, L was selected as 1m and B as 2.3×10^{15}m/V^2, then E_m was 14.74 kV/mm. Combining equations (1) and (2), the strength of the applied electric field could be calculated [12].

As the light intensity changes with the electric field, when the strength of applied electric field exceeds E_m, the light intensity will appear peak values twice at both the wave-front stage and wave-tail stage during the impulse voltage application, as shown in Figure 1.

For convenience of description, the amplitude of applied voltage corresponding to the peak light intensity at the

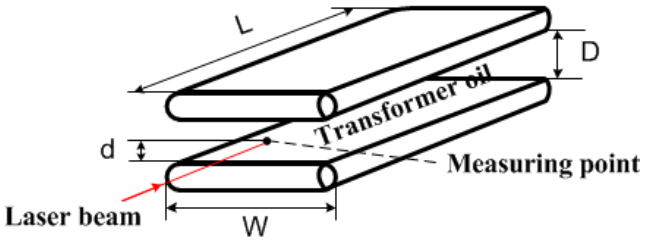

FIGURE 2. Test model.

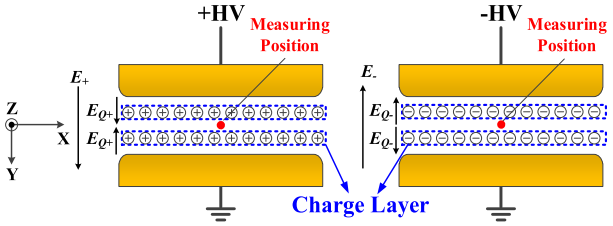

FIGURE 3. Schematic diagram of equivalent charge layers.

wave-front stage is noted as U_h, and the corresponding time when the peak value of light intensity appears is noted as P_h. The amplitude of applied voltage corresponding to the peak light intensity at the wave-tail stage is marked as U_t, and the corresponding time is marked as P_t. In the absence of space charge in the oil, U_h should equals to U_t.

The experimental platform adopted in this paper is designed in our former study, the minimum sensitivity of the platform was 3.5 kV/mm and the maximum deviation was 3.6% [12]. The test model applied in this paper is also the same one as used in our previous research [12], which is composed of two parallel plate electrodes with the spacing D of 5 mm. As shown in Figure 2, for the electrode, the length L was 1 m, the width W was 80 mm, the surface evenness was less than 0.1 mm, and the surface degree of finish was 1.6 μm. The incident point of the single-wavelength laser beam was located in the middle of the two electrodes.

Between the electrodes was filled with transformer oil, which was filtered for purity, dehydrated and degassed for 48 hours under 85°C vacuum conditions. The content of moisture in the processed oil was recorded as 7.98-8.27 μL/L, which meets the requirements of the relevant standards [13].

As show in Figure 3, the single-point laser incidence was adopted for the electric field measurement, in consequence, the electric field at the measuring position is the combined field generated by both the applied impulse electric field and the space charges in the oil.

All the charges in the oil can be equivalent to the surface charges on the XZ plane where the light beam is located. The difference in the motion velocity of charge carriers along the Y direction may form a non-uniform distribution of charges whilst the XZ plane appears uniform distribution of the charges. Therefore, the charge distribution in the oil gap between the electrodes can be viewed as many charge layers, and the overall polarity of each charge layer is depended on the comparison of the number of positive and negative charges. If the measured electric field is smaller than the applied impulse field, the charges on the plane would be equivalent as positive charges. On the opposite, the charges on the plane would be equivalent as negative ones. Using the Gauss' flux theorem, the equivalent charge density in the Gauss surface can be obtained as follows.

$$\oint_S E_Q \cdot \mathrm{d}s = \frac{Q}{\varepsilon_r \varepsilon_0} \tag{3}$$

In equation (3), Q denotes the total quantity of electric charges in the Gaussian surface, S represents the area of the Gaussian surface, ε_r marks the relative permittivity of the dielectric medium, and $\varepsilon_0 = 8.85\times10^{-12}$F/m represents the vacuum permittivity.

Given that the diameter of the laser beam (1mm) is much smaller than the width of electrode (80 mm), the laser incident plane that is parallel to the electrodes (XZ plane) can be regarded as an infinite evenly charged surface close to the measuring position. The surface charge density is marked as σ, and generates the electric fields E_Q, as shown in Figure 3. The bidirectional closed cylindrical surface is taken as the Gaussian surface and the equation (4) can be obtained from the symmetry of the model. Then, the equivalent charge density of the charge layer can be obtained by equation (5).

$$2E_Q \Delta S = \sigma \Delta S / (\varepsilon_r \varepsilon_0) \tag{4}$$

$$\sigma = 2\varepsilon_r \varepsilon_0 E_Q \tag{5}$$

III. CHARACTERISTICS OF ELECTRIC FIELD IN OIL UNDER IMPULSE VOLTAGE

The present paper measured the dynamic characteristics of electric field in transformer oil under impulse voltage. Different electrode materials, voltage amplitudes, wave-front times as well as different positions of measuring points were examined to have captured the correspondent changes of electric field.

A. INFLUENCE OF ELECTRODE MATERIALS

The electrode materials used in the present paper were copper (Cu), aluminum (Al), and stainless steel (Fe) respectively. As for the ease of description, element symbol combination of is employed to represent the corresponding electrode combination, for instance, Cu -Al stands for the upper electrode is made of copper, and the lower one is made of aluminum. Standard lighting impulse voltage with front time of 1.2 μs, half-value time of 50 μs and peak value of +100 kV was applied to each of the electrode combinations [14].

The experimental results are shown in Figure 4, it can be seen that the theoretical peak value of the applied electric field was 20 kV/mm and the measured peak value of the Cu-Cu, Al-Al, and Fe-Fe electrode combinations were 18.05 kV/mm, 16.12 kV/mm, and 14.20 kV/mm respectively. The electric field strength under Al-Al electrode combination was higher than that under Cu-Cu combination by 19.25%.

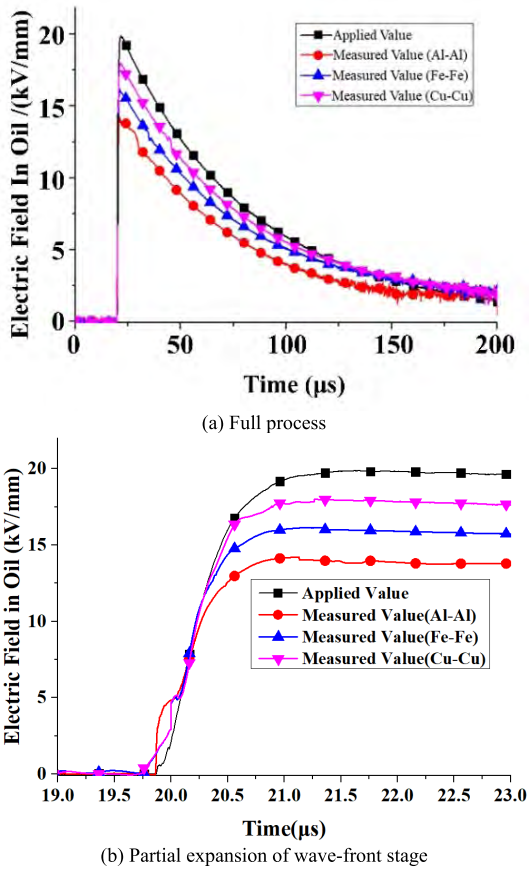

(a) Full process

(b) Partial expansion of wave-front stage

FIGURE 4. Variation of electric field in oil under different electrode combinations.

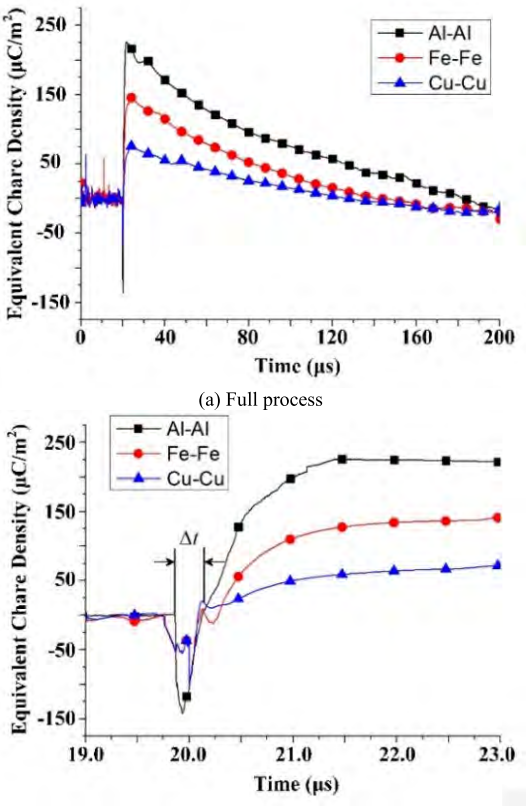

(a) Full process

(b) Partial expansion of wave-front stage

FIGURE 5. Variation of charges in oil under X-X electrode combination.

The changes of the equivalent charge density at the measuring position over time for the three electrode combinations are shown in Figure 5. The average equivalent charge densities density of Al-Al, Fe-Fe, and Cu-Cu electrode combination was 68.4 μC/m^2, 32.7 μC/m^2, and 13.3 μC/m^2 respectively.

The Al-Al electrode combination had the largest quantity of injected charge whilst the Cu-Cu combination had the least. There exists huge differences in the charge injection amount from the different metal electrodes under the same voltage, which could be attributed to the facts that the work functions of the metals, namely the required energy for an electron to jump from the Fermi level to the lowest energy level (vacuum level), are different. Under the normal circumstances, the metal atoms are much more active than the organic molecules in a dielectric under the action of an electric field. On the interface between metal and oil, the Fermi level would approaching the conduction band, which means that the density of free carrier near the interface could be higher than that in the bulk, and a carrier accumulation layer on the interface would be formed. Due to the fact that, the work function of the metal is lower than that of the dielectric, the electrons are more likely to be injected into the dielectric from the metal, and the smaller the work function of the metal, the easier it is to inject. As for the work function of Cu, Fe, and Aluminum, it reads as 4.47 eV, 4.36 eV, and 3.74 eV respectively [15], consequently, the Al-Al combination is easy to inject charges and Cu-Cu combination is much harder.

In order to further explore the effect of the space charge on the electric field characteristics in the oil, the cross electrode combinations tests under the same conditions were preformed, namely X-Y electrode combination, as shown in Figure 6.

It could be obtained that in the case of X-Y electrode combinations, whether the copper was set as the upper electrode or the lower one, it always revealed that the aluminum electrode witnessed the biggest impact of space charge on electric field, followed by the stainless steel and then the copper. It is generally agreed that the charge carriers in transformer oil are positive ions, negative ions, and electrons. While in the concerned of experimental results in this paper, it takes many milliseconds for either the positive or negative ions to pass the 5 mm spacing with a migration rate of 10^{-9} m^2/ (V·s) [15], even when they perform continuous acceleration motion under the electric field strength of 20 kV/mm. This cannot interpret the measurement results under the lightning impulse voltage. Due to the faster mobility of electrons, namely 10^{-4} m^2/(V·s) [15], it only takes a few

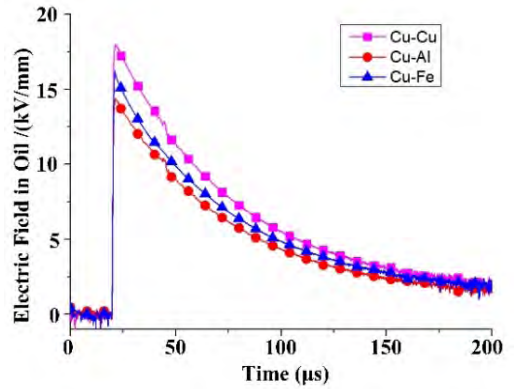

(a) Cu-X electrodes combinations

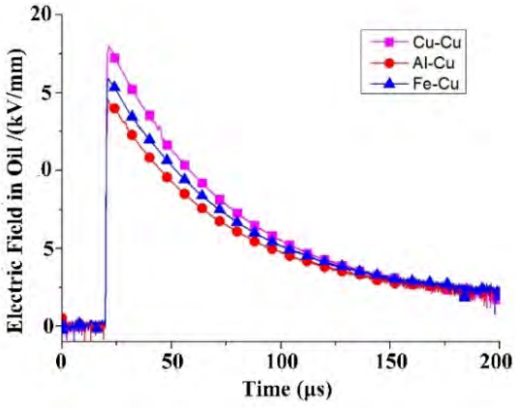

(b) X-Cu electrodes combinations

FIGURE 6. **Variation of electric field in oil under X-Y electrode combination.**

milliseconds (μs) for electrons to pass the 5 mm oil spacing, which is very close to the measurement results in this paper. As a consequence, the electrons are concluded as the major negative charges in the oil under impulse voltage, and this will be deeply discussed in Section 4.

B. INFLUENCE OF VOLTAGE AMPLITUDE

In order to simulate the actual operating conditions in transformer, the design curves of the electric field in oil gaps proposed by Weidmann were taken into consideration, which indicated that the allowable field strength for 5mm oil gap under impulse voltage should be about 22.8kV/mm [16-17]. In consequence, the impulse voltages with positive amplitude (peak value) of 75 kV, 83 kV, 95 kV and 100 kV and wave-front time of 1.2 μs were applied to the test model with Cu-Cu type electrode system. The relationship between applied electric field and measured one under +100 kV impulse voltage is shown in Figure 7, but from which it is difficult to present the influence of voltage amplitude on electric field or charge characteristics. In consequence, for the convenience of better discussion and clearer presentation, the relationship between applied voltage and light intensity, and the corresponding parameters mentioned in Section 2, namely E_m, U_h, P_h, U_t and P_t are adopted in the following discussion.

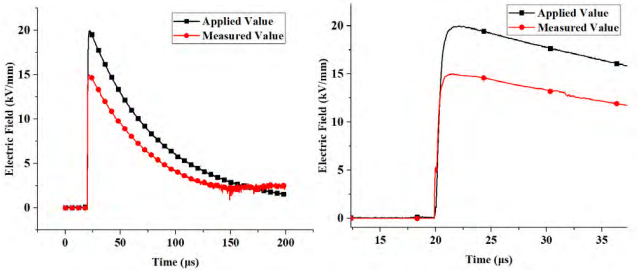

(a) Full process (b) Partial expansion of wave-front stage

FIGURE 7. **The relationship between the applied electric field and measured one under 100kV impulse voltage.**

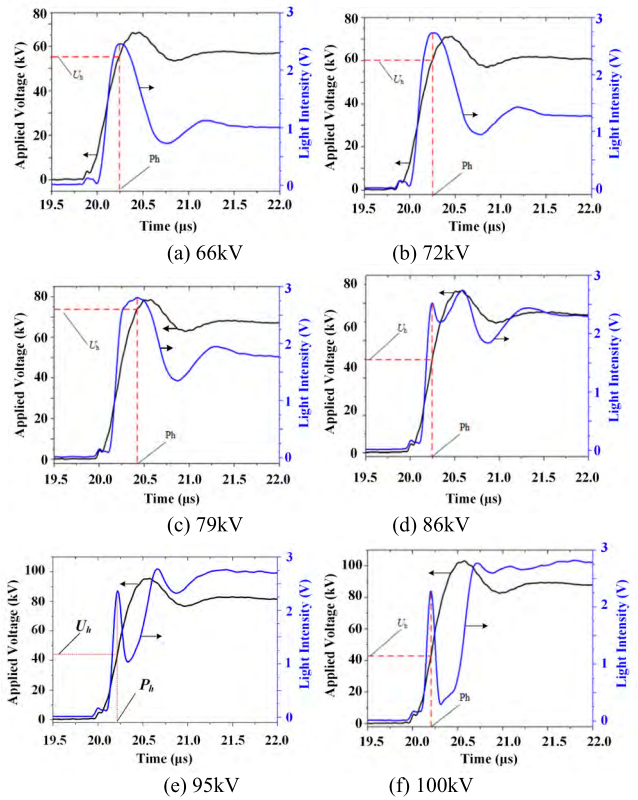

(a) 66kV (b) 72kV

(c) 79kV (d) 86kV

(e) 95kV (f) 100kV

FIGURE 8. **The relationship between the applied voltage and the light intensity under different amplitude of impulse voltage.**

The relationship between the light intensity and the applied voltage at the wave-front stage is shown in Figure 8. The short front waveform is generated from the sphere-gap discharge by a small wave-front resistance, which is relatively violent and thus results the overshoot in the waveform of impulse voltage. However, it is still within the range of acceptable limit specified in IEC standard [14] and thus does not affect the discussion of the measurement results.

As is shown in Figure 8, despite the differences of U_h values under different amplitudes of impulse voltage, the change of P_h is rather small. Table 1 presents the statistics in this regard.

Under the condition of electrode spacing of 5 mm, if there is no space charge in the oil, the voltage value at the first peak

TABLE 1. U_h and P_h under different amplitude of impulse voltage.

Amplitude of impulse Voltage /kV	U_h / kV	P_h / ns
66.00	55.30	238
72.00	59.31	255
79.00	75.07	278
86.00	50.60	245
95.00	44.90	221
100.00	42.40	203

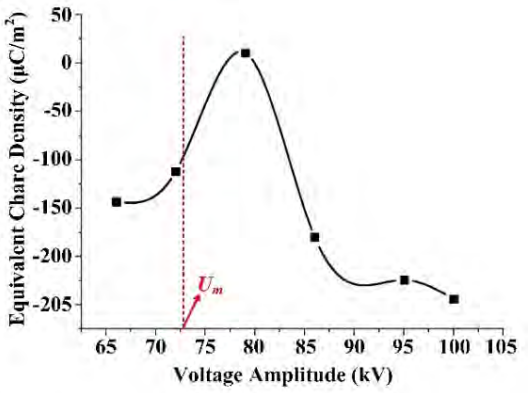

FIGURE 9. The change of the equivalent charge density with the voltage amplitude at Ph time point.

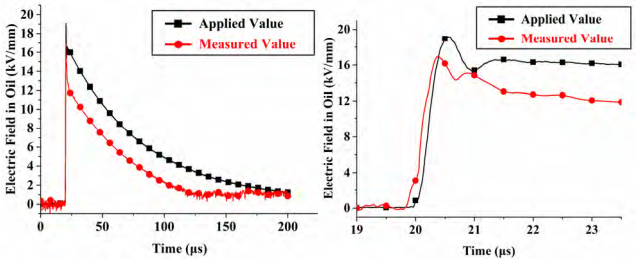

(a) Full process (b) Partial expansion of wave-front stage

FIGURE 10. The electric field in oil under voltage with wave-front time of 0.5 μs.

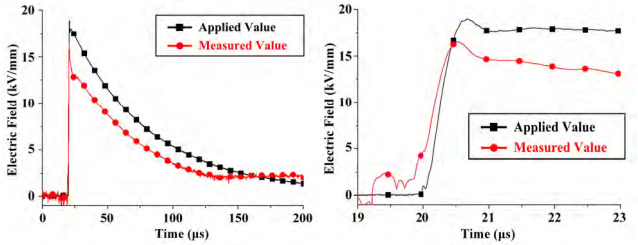

(a) Full process (b) Partial expansion of wave-front stage

FIGURE 11. The electric field in oil under voltage with wave-front time of 0.7 μs.

light intensity would be $U_m = 5 \times E_m = 73.70$ kV. However, it can be obtained from Table 1 that with the increase of amplitude, U_h first increased and then decreased. U_h exceeded U_m and reached its peak value as the impulse voltage mounted up to 79.00 kV, after which U_h gradually decreased. This shows that as the voltage amplitude increases, the space charge firstly enhances, then weakens, and again enhances the intermediate electric field in the oil gap. Figure 9 presents the change of the equivalent charge density with the voltage amplitude at the time point P_h.

The negative charges injected into the oil by the cathode under high electric field are electrons generated by field emission. The process of these negative charges moving towards the anode can be approximately considered as a variable acceleration motion, which is much more complicated than the uniform acceleration motion under DC voltage, the relationship between applied voltage and speed of negative charges could be explained as follows:

1) When the amplitude of impulse voltage is low (e.g. 66 kV, 72 kV), the acceleration of electrons is relatively small, the initial speed of electrons is relatively slow and they cannot reach the measuring position in the middle of the test model. Therefore, the space charge field enhances the electric field in the oil, as a result of which the light intensity will observe a peak value even if the applied voltage does not reach U_m (73.70 kV).

2) When the amplitude of impulse voltage is high (e.g. 86 kV, 95 kV and 100 kV), the voltage rises quickly. Although the acceleration of electrons gets greater, the speed of charge is unable to keep up with the increase of applied voltage. Without adequate electrons accumulation in the vicinity of the anode, the space charge continues to enhance the electric field, and the light intensity will also reach its peak value even if the applied voltage does not reach U_m (73.70 kV).

3) The voltage amplitude has a critical value (i.e. 79 kV in this test setup), under which there is adequate electrons accumulation in the vicinity of the anode at the time point P_h. As a result, the impact of positive and negative charges on the electric field at the measuring point counteracts each other, and the measured strength electric field is close to the applied one.

C. INFLUENCE OF WAVE-FRONT TIME

According to the voltage selection method described in Section III.B, in this test, the amplitude of impulse voltage was kept constant at +95 kV and the wave-front time being adjusted to 0.5 μs, 0.7 μs, 2.0 μs, 7.0 μs, 10.0 μs, 25.0 μs, and 40.0 μs respectively, and the electrode system is Cu-Cu. The comparison of applied value and measured value of electric field in oil under impulse voltage with various wave-front times are shown in Figure 10 to Figure 16.

Figure 17 presents the variation of the peak value of measured electric field with wave-front time. It was found that, the peak value of the measured electric field could gradually decrease by 17.6% when the wave-front time increased from 0.5 μs to 40.0 μs.

The results in Figure 17 could be explained that, the longer the wave-front time is, the longer time the electric field will keep in high amplitude, the greater amount of charge will be injected into the oil by the electrode, and the greater

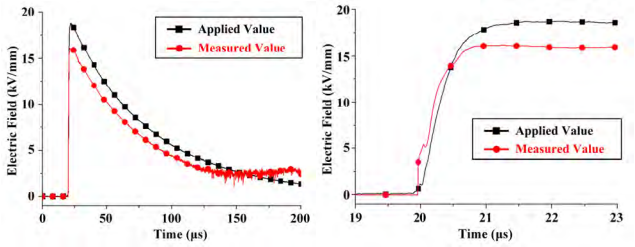

(a) Full process (b) Partial expansion of wave-front stage

FIGURE 12. The electric field in oil under voltage with wave-front time of 2.0 μs.

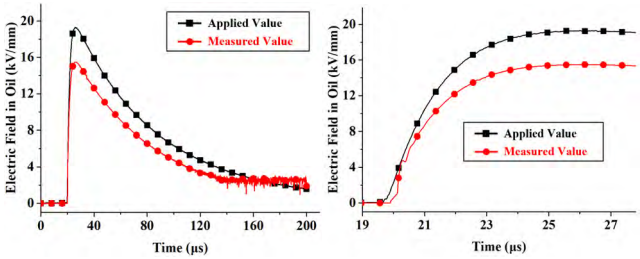

(a) Full process (b) Partial expansion of wave-front stage

FIGURE 13. Comparison of applied value and measured value of electric field in oil under wave-front time of 7.0 μs.

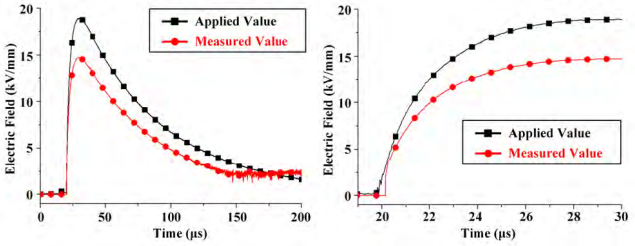

(a) Full process (b) Partial expansion of wave-front stage

FIGURE 14. Comparison of applied value and measured value of electric field in oil under wave-front time of 10.0 μs.

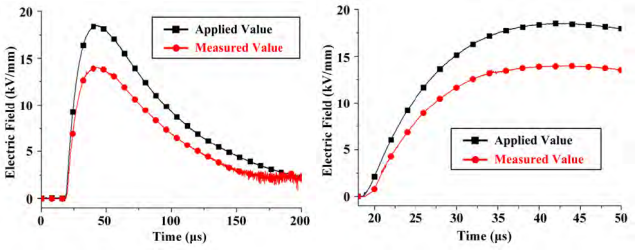

(a) Full process (b) Partial expansion of wave-front stage

FIGURE 15. Comparison of applied value and measured value of electric field in oil under wave-front time of 25.0 μs.

the weakening effect of the applied electric field will be. In order to make a quantitatively explanation, the P_h and P_t were induced to present the variation of equivalent charge density at P_h and P_t with different wave-front time, as shown in Figure 18. It could be found that, with the wave-front time increasing, the equivalent charge polarity changed from

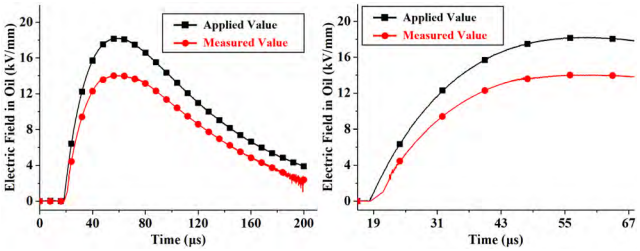

(a) Full process (b) Partial expansion of wave-front stage

FIGURE 16. Comparison of applied value and measured value of electric field in oil under wave-front time 40.0 μs.

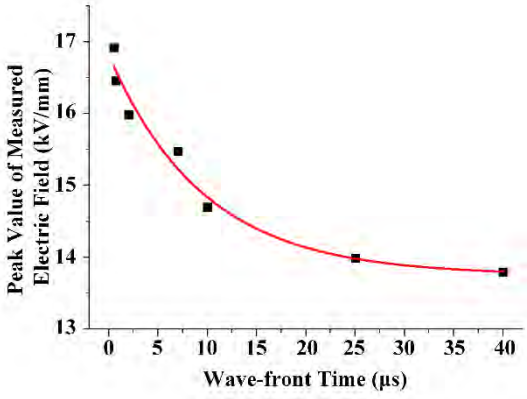

FIGURE 17. The variation of the peak value of measured electric field with wave-front time.

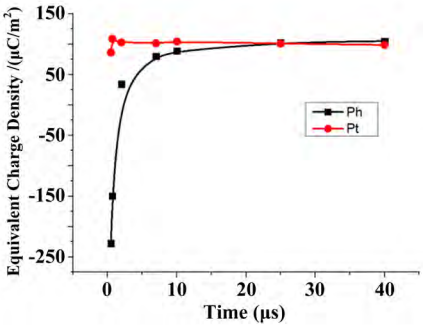

FIGURE 18. The variation of equivalent charge density at P_h and P_t with different wave-front time.

negative to positive, which means the more wave-front time provided more time for the charge generation.

D. INFLUENCE OF SPATIAL POSITIONS

Under the standard lightning impulse voltage with peak value of +90 kV, the spatial distribution of electric field in Cu-Cu electrode combination in oil was measured, as shown in Figure 19, in which the positive directions of X and Y axis are defined. Five measuring positions were set from the top electrode to the bottom one. The top-down scan was performed by a set of high-precision motor driving system, which could drive the laser, polarizer, alignment unit, quarter-wave plate,

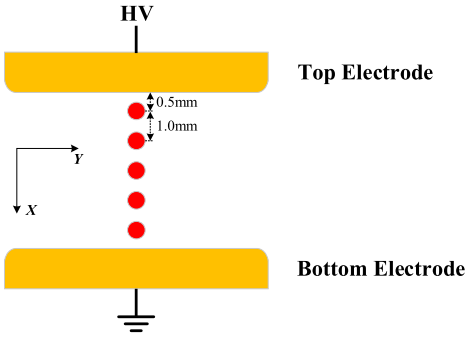

FIGURE 19. Spatial distribution of measuring positions.

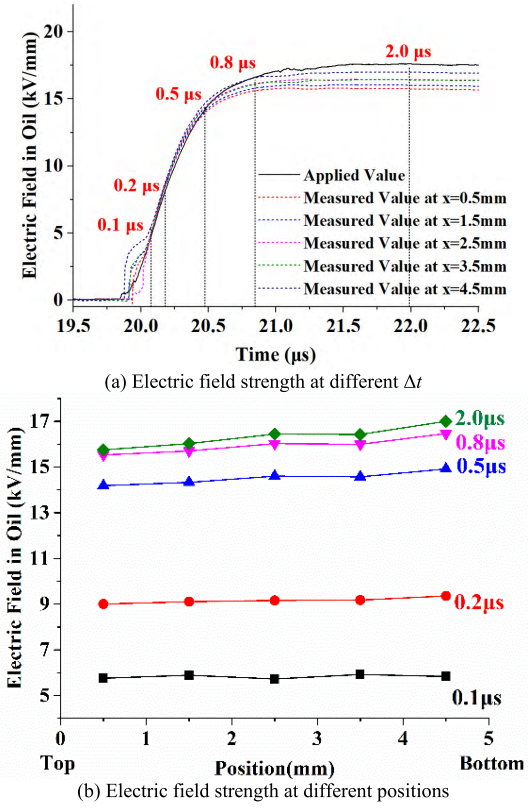

(a) Electric field strength at different Δt

(b) Electric field strength at different positions

FIGURE 20. Spatial distribution of electric field.

analyzer and photodetector to move up and down linearly in Y direction [9]. The surface of the top electrode is set as the origin of X-axis and the coordinates of the five measuring positions are x = 0.5 mm, 1.5 mm, 2.5 mm, 3.5 mm and 4.5 mm respectively. Figure 20 shows the electric field distribution at different locations of $\Delta t = 0.1\mu$s, 0.2 μs, 0.5 μs, 0.8 μs and 2.0 μs.

The spatial distribution of electric field shows that the electric field between the top and bottom electrodes is quite uniform at the stage of initial application of the impulse voltage ($\Delta t = 0.1\mu$s, 0.2μs). As the voltage gradually increases ($\Delta t = 0.5\mu$s), the slope of the electric field strength with the position increases gradually, and the electric field near the top and the bottom electrodes appears an

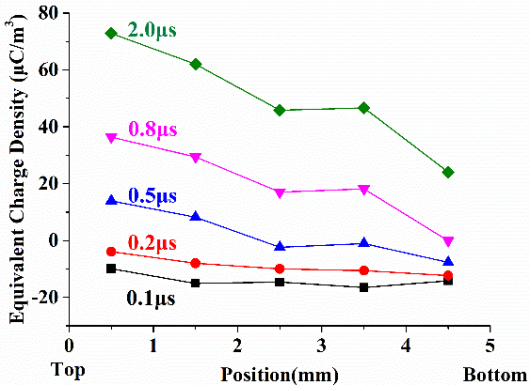

FIGURE 21. Spatial distribution of equivalent charge density.

asymmetric distribution. When the impulse voltage mounts to the peak ($\Delta t = 0.8\mu$s, 2.0μs), the electric field near the bottom electrode is slightly higher than that near the top one. The equivalent charge density can be calculated from the difference between the measured strength of electric field and the applied one. The spatial distribution of the equivalent charge density at the five measuring positions of $\Delta t = 0.1\mu$s, 0.2μs, 0.5μs, 0.8μs and 2.0μs is shown in Figure 21.

It can be seen that at the time of $\Delta t = 0.1\mu$s and 0.2μs, the equivalent charge densities between the electrodes are both negative, indicating that the space charge fields are in the same direction as the applied field and play the enhancing roles. At the time of $\Delta t = 0.5\mu$s, the charge density near the top electrode is positive whilst that near the bottom is negative, indicating that the charge is in the dynamic motion process and it affects the electric field in an enhancing manner at first and then in a weakening manner. At the time of $\Delta t = 0.8\mu$s or 2.0 μs, the equivalent charge densities between the electrodes are positive, indicating that the space charge fields are opposite to the applied field and exert weakening effects.

IV. MODEL OF SPACE CHARGE MOTION IN OIL UNDER IMPULSE VOLTAGE

A. CHARGE INJECTION MECHANISM

According to the theory of field ionization, the contact between the metal electrode and the dielectric is Ohmic contact. As the work function of the metal φ_m is much smaller than that of the dielectric φ_d, the Fermi level at the interface approaches to the conduction band, and the free carrier density is much higher at/near the contact place than in the body. The interface constitutes a carrier-accumulating layer, and the metal electrode injects electrons into the dielectric. Schottky emission is a thermal emission that has certain temperature requirements. However, experiments have shown that when the electric field reaches 1% of E_c, i.e. 10^8V/m, even if the temperature is low, the non-Ohmic current in the dielectric is already quite obvious, and electrons can still enter the dielectric as the tunneling effect to generate field emission.

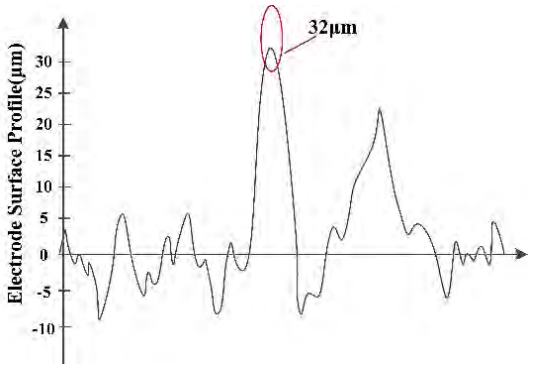

FIGURE 22. Microscopic profile of electrode surface.

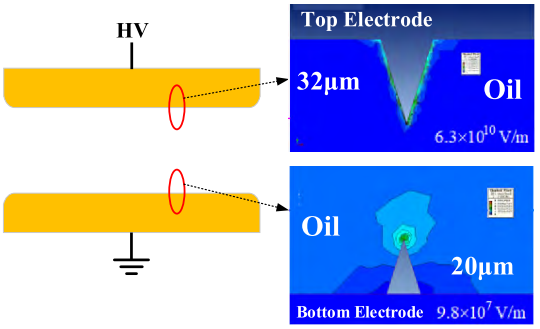

FIGURE 23. Simulation results of local electric field on electrode surface.

The peak value of the impulse electric field applied in this experiment was 0.2×10^8V/m. However, the electrode surface is not completely smooth and there are many tips and burrs, as a result of which the local electric field strength on the electrode surface may exceed the electron emission field strength of 10^8V/m. The ZYGO white light interferometer was adopted to perform a three-dimensional scan on surface profile of the 6.0 μm$\times$ 6.0 μm region on the electrode. As shown in Figure 22, the electrode surface demonstrates many tips and protrusions with an average undulation height of 3.2 μm and a maximum height of 32.0 μm.

Modeling this shape of tip as an isosceles triangle in Infolytica simulation software, the electric field around it was simulated and calculated under the experimental conditions. The results are shown in Figure 23. At 300 ns, the local electric field near the tip of the top electrode surface reached 6.3×10^{10}V/m, exceeding the field emission field strength. The local electric field near the tip of the bottom electrode surface was 9.8×10^7V/m, which was also relatively close to the field emission field strength.

It is inferred that, under the aforementioned electric field conditions, the negative charges in the transformer oil are the electrons injected by the bottom electrode (cathode) and the electrons may combine with the neutral molecules to form negative ions during the movement to the anode. Reference [18] reported the mobility of electrons in certain nonpolar liquid, such as the electron mobility in Neopentane (C_5H_{12}) being up to 6.5×10^{-3}m^2/(V·s).

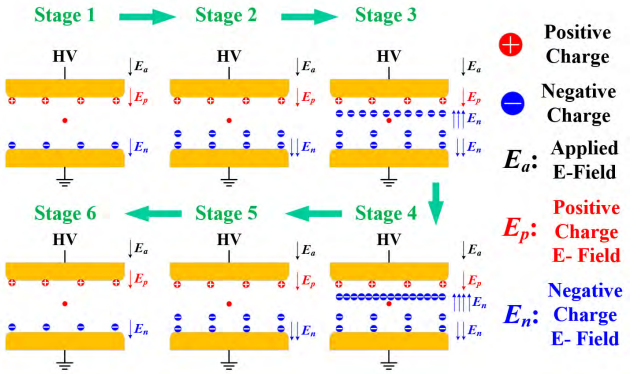

FIGURE 24. Space charge motion model in transformer oil.

At the top electrode (anode), also due to the high local field strength produced by the tips and protrusions on the electrode surface, electrons in the lower energy levels of the neutral oil molecules near the electrode are excited by the electric field to obtain higher energy, transit to the high energy level, and become free electrons to escape from molecules. The originally neutral oil molecules became positive ions. In addition, transformer oil contains trace amounts of acids, nitrides, oxides, and oxygen. Electrochemical reactions will happen when metal electrodes come into contact with them, producing Cu^{2+}, Fe^{2+}, Al^{3+} and other metal ions, which could easily escape from the metal into the oil under the action of the electric field. Both the positive ions produced by the ionization of oil molecules and the metal ions produced by electrochemical reactions of electrodes constitute the sources of positive charges in the oil. Since the mass of positive ions is much greater than that of the electrons, the negative charge moves faster than the positive charge under the application of electric field.

B. CHARGE MOTION MECHANISM

Based on the measured electric field characteristics in oil under impulse voltage and their relationship with electrode material, voltage amplitude and wave-front time, the space charge motion process in oil can be divided into the following six stages during the voltage application, as shown in Figure 24.

Stage 1- During the stage of voltage rising, in spite of relative low electric field, the electrons can be injected into oil from the electrode due to the tunneling effect, and then distributes in the area very close to the surface of the cathode. While for the area close to surface of anode, the oil molecules lost their electrons to become positive ions under the action of applied electric field. In addition, the metal ions injected from the electrodes could make supplement to the space charges near anode. In the oil gap, which could be considered as the charge electrets of same charge polarity, the formed space charge field could strength the applied electric field. Meanwhile, the ever-increasing field strength could force

the charges to make directional motions along the electric field line.

Stage 2- The electrons are of lighter mass and can migrate across the molecules, while as for the positive charges with the larger mass, the obtained initial kinetic energy could not force them to make motions. In addition, the motion speed of negative charge is much greater than the positive charge. Therefore, under the application of impulse voltage in this stage, the electrons start to make accelerated movement towards the anode while the positive charges will still stay near the anode.

Stage 3- The oil molecules near the anode are ionized into positive ions and electrons. Due to the attraction of positive ions, the electrons could form a shielding layer outside the positive charge layer. When the negative charge moved near to the anode, due to the repulsion of the shielding layer, its speed is greatly reduced, and the neutralization process with the positive charge is also slowed. Parts of the electrons are combined with neutral molecules to become negative ions, and then they accumulate to form a negative charge layer. As the amount of negative charge increases, it exerts weakening effect on the electric field in the oil and the measured electric field begins to be lower than the applied electric field.

Stage 4- With the voltage application prolonging, the bigger the amount of negative charge layers become, the lower the electric field at the measuring position will be than the applied electric field. When the applied voltage boosts close to the peak value, both the charge injection rate and the charge neutralization rate reach a relatively balanced state, and the space charge could exert the maximum weakening effect on the applied electric field.

Stage 5- After the peak value, the amplitude of applied voltage begins to decrease, and the amount of charge injection therewith decreases. Due to neutralization process, the amount of positive and negative charges is greatly reduced. The head region of the negative charge gradually retreats toward the cathode.

Stage 6- During the wave tail stage of voltage decreasing, the charge injected by the electrode is greatly reduced. At the same time, the positive and negative charges in the oil gap are also exhausted due to the neutralization process. The charge distribution returns to the initial state when there is a small amount of positive charge near the anode and also a small amount of negative charge near the cathode. The space charge field exerts an enhancing impact on the electric field at the measuring position.

C. MOBILITY OF ELECTRON

As the charge motion process shows in Figure 24, after the electron injection from the cathode electrode, the electron starts to move towards the measuring position. The electric field induced by electron, namely electron field in the followings, could exert an enhanced effect on the electric field of measuring position before the electron arrives at the measuring position. When the electron reaches the position very close to measuring position, the compound electric field superimposed by both electron field and applied electric field appears the maximum field strength. When the electron passes cross the measuring position, the electron field has the opposite direction to the applied field at the measuring position, and then the charge field begins to fall. Therefore, the mobility of electron could be obtained through the equation (6):

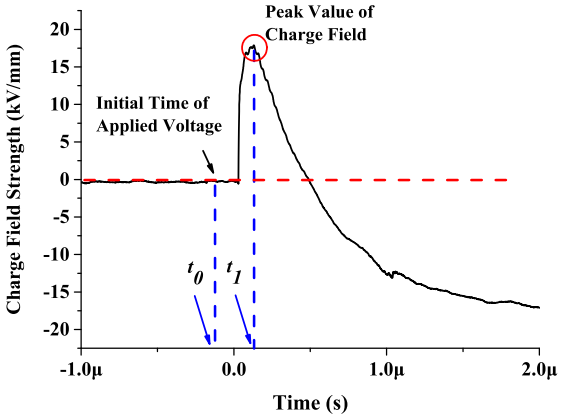

FIGURE 25. The charge field strength.

$$\mu = \frac{d}{(t_1 - t_0) \cdot E} \tag{6}$$

in which, d stands for the distance between measuring positions or the distance between ground electrode and measuring position, t_0 represents initial time of voltage application, t_1 marks the time of charge field strength reaching maximum, and E is the measuring electric field strength. The equation (6) indicated the electric field strength could exert a significant effect on the electron mobility, while during the application of impulse voltage, the applied field strength is always changing. The captured electron mobility is this paper was regarded as the equivalent one during the time difference between t_0 and t_1.

The charge field could be worked out by the difference between measuring electric field strength and applied electric field strength, as shown in Figure 25.

1) THE INFLUENCE OF VOLTAGE AMPLITUDE ON ELECTRON MOBILITY

Referring to the experimental results in Section 3.2, the voltage-amplitude dependent electron mobility is shown in Figure 26. In this case, the d is 2.5 mm, $\Delta t = (t_1\text{-}t_0)$ is the time interval from voltage beginning to the maximum charge field strength, and E marks the measuring electric field.

It could be indicated from Figure 25 that, with the voltage amplitude increasing, the electron mobility tends to decrease, and the maximum reduction percentage could reach 16.7%.

2) THE INFLUENCE OF WAVE-FRONT TIME ON ELECTRON MOBILITY

The experimental results in Section 3.3 indicated that, only in the cases of wave-front time of 0.5 μs, 0.7 μs and 2.0 μs,

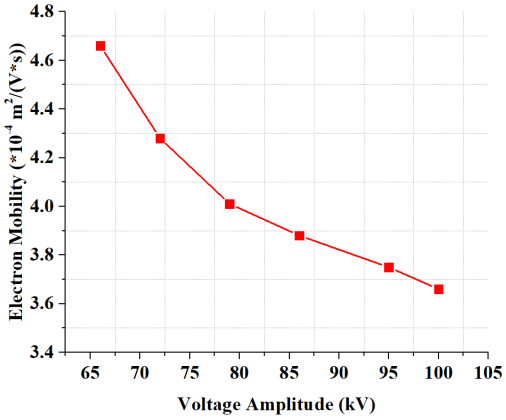

FIGURE 26. The influence of voltage amplitude on electron mobility.

TABLE 2. The variation of electron mobility over wave-front time.

Wave-front Time / μs	Electron Mobility / *10^{-4} m^2/(V*s)
0.5	4.75
0.7	4.82
2.0	4.77

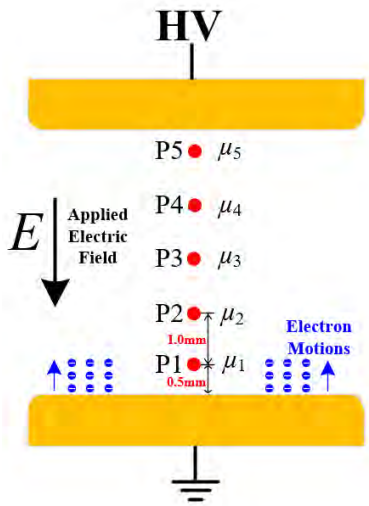

FIGURE 27. The different measuring positions.

the excess of measured electric field strength on applied one could be witnessed. Though, when the wave-front time is beyond 2.0 μs, due to the limitation of measuring platform, such excess could not be captured.

Table 2 illustrates the variation of electron mobility over wave-front time, telling that, the wave-front time could exert rare effect on the electron mobility.

3) THE SPATIAL CHARACTERISTICS OF ELECTRON MOBILITY

In the concerned of electron mobility in different position along its motion path from ground electrode to HV electrode, Figure 25 can demonstrate the schematic diagram for

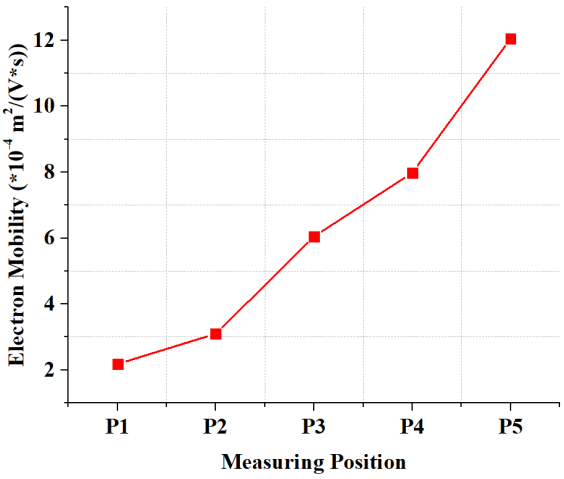

FIGURE 28. The spatial characteristics of electron mobility.

analysis and calculation. In Figure 27, μ_1 stands for the electron mobility at the P1 measuring position, in this case, d = 0.5 mm, $\Delta t = (t_1 - t_0)$ is the time interval from voltage beginning to arriving time of electron reaching P1, and E marks the average electric field strength during this interval. By that analogy, the electron mobility at each measuring position could be captured, as shown in Figure 28.

From the experimental results, it could be indicated that, the closer the electron gets to the high voltage electrode, the faster the mobility.

V. CONCLUSION

In this paper, the temporal-spatial distribution characteristics of electric field in transformer oil under impulse voltage with various test conditions is measured, and based on which, the space charge motion model is also proposed. The following conclusions can be drawn.

1) Under the lightning impulse voltage, the amount of charge injection with aluminum electrode is the largest, followed by stainless steel and copper. This is attributed to the work function (Al<Fe<Cu) of the metal elements contained in the three electrodes.

2) With the increase of the voltage amplitude, the effect of the space charge on the electric field of the oil gap is enhanced at first, then weakened and again enhanced.

3) As the wave-front time prolongs, the peak of electric field in transformer oil shows a downward trend. For instance, the peak value of the electric field is reduced by 17.6% when the wave-front time is increased from 500 ns to 40 μs.

4) Adopting the field emission and field-induced ionization theory, the sources of negative and positive charges in the transformer oil are explained respectively. In addition, the charge motion laws under the application of impulse voltage are also proposed. During the process of the impulse voltage application, the charge has a dynamic movement process, and the different positions of charges at different moments could lead to different effects on the electric field. The space

charges could firstly exert a weakened effect on the electric field strength and then make an enhanced contribution.

5) The electron mobility was also worked out in this paper to present the quantitative results of its motion process. With the increase in voltage amplitude, the electron mobility tends to decrease, and the maximum reduction percentage can reach 16.7%, while the different wave-front time could exert rare effect on the electron mobility. For the variations electron mobility with spatial position, it is found that the closer the electron gets to the high voltage electrode, the faster the mobility.

REFERENCES

[1] G. Ueta, T. Tsuboi, J. Takami, and S. Okabe, "Insulation characteristics of oil-immersed power transformer under lightning impulse and AC superimposed voltage," *IEEE Trans. Dielectr. Electr. Insul.*, vol. 21, no. 3, pp. 1384–1392, Jun. 2014.

[2] M. J. Heathcote, *J & P Transformer Book*, 12th ed. Oxford, U.K.: Newnes, 1998, pp. 398–407.

[3] Y. Kamata, A. Miki, and S. Furukawa, "A singular flashover path observed on the surface of synthetic-resin-bonded paper cylinders immersed in transformer oil under switching impulse voltage conditions," *IEEE Trans. Electr. Insul.*, vol. 26, no. 2, pp. 300–310, Apr. 1991.

[4] E. C. Cassidy, R. E. Hebner, M. Zahn, and R. J. Sojka, "Kerr-effect studies of an insulating liquid under varied high-voltage conditions," *IEEE Trans. Electr. Insul.*, vol. EI-9, no. 2, pp. 43–56, Jun. 1974.

[5] M. Zahn, Y. Ohki, K. Rhoads, M. LaGasse, and H. Matsuzawa, "Electro-optic charge injection and tramsport measurements in highly purified water and water/ethylene glycol mixtures," *IEEE Trans. Electr. Insul.*, vol. EI-20, no. 2, pp. 199–211, Apr. 1985.

[6] A. Helgeson and M. Zahn, "Kerr electro-optic measurements of space charge effects in HV pulsed propylene carbonate," *IEEE Trans. Dielectr. Electr. Insul.*, vol. 9, no. 5, pp. 838–844, Oct. 2002.

[7] F. O'Sullivan, S.-H. Lee, M. Zahn, L. Pettersson, R. Liu, O. Hjortstam, T. Auletta, and U. Gafvert, "Modeling the effect of ionic dissociation on charge transport in transformer oil," in *Proc. IEEE Conf. Elect. Insul. Dielectric Phenomena*, Kansas City, MO, USA, Oct. 2006, pp. 756–759.

[8] W. Sima, H. Song, Q. Yang, H. Guo, M. Zahn, and M. Yang, "Time-continuous Kerr electro-optic field mapping measurement under impulse voltage using array photodetector," *Appl. Phys. Lett.*, vol. 107, no. 8, 2015, Art. no. 082901.

[9] B. Qi, X. Zhao, C. Li, and H. Wu, "Electric field distribution in oil-pressboard insulation under AC-DC combined voltages," *IEEE Trans. Dielectr. Electr. Insul.*, vol. 23, no. 4, pp. 1935–1941, Aug. 2016.

[10] B. Qi, X. Zhao, C. Li, and H. Wu, "Transient electric field characteristics in oil-pressboard composite insulation under voltage polarity reversal," *IEEE Trans. Dielectr. Electr. Insul.*, vol. 22, no. 4, pp. 2148–2155, Aug. 2015.

[11] B. Qi, C. Gao, X. Zhao, C. Li, and H. Wu, "Interface charge polarity effect based analysis model for electric field in oil-pressboard insulation under DC voltage," *IEEE Trans. Dielectr. Electr. Insul.*, vol. 23, no. 5, pp. 2704–2711, Oct. 2016.

[12] B. Qi, X. Zhao, S. Zhang, M. Huang, and C. Li, "Measurement of the electric field strength in transformer oil under impulse voltage," *IEEE Trans. Dielectr. Electr. Insul.*, vol. 24, no. 2, pp. 1256–1262, Apr. 2017.

[13] *Fluids for Electrotechnical Applications—Unused Mineral Insulating Oils for Transformers and Switchgear*, Standard IEC 60296-2012, 2012.

[14] *High-Voltage Test Techniques—Part 1: General Definitions and Test Requirements*, Standard IEC 60060-1-2010, 2010.

[15] Z.-R. Peng, R.-S. Liu, and D.-M. Tu, "Investigation into dynamic process of space charge in liquid dielectrics using the Kerr-effect technique," in *Proc. 3rd Int. Conf. Properties Appl. Dielectric Mater.*, Tokyo, Japan, Jul. 1991, pp. 276–279.

[16] J. K. Nelson and C. Shaw, "The impulse design of transformer oil-cellulose structures," *IEEE Trans. Dielectrics Electr. Insul.*, vol. 13, no. 3, pp. 477–483, Jun. 2006.

[17] K. J. Rapp, J. Corkran, C. P. Mcshane, and T. A. Prevost, "Lightning impulse testing of natural ester fluid gaps and insulation interfaces," *IEEE Trans. Dielectrics Electr. Insul.*, vol. 16, no. 6, pp. 1595–1603, Dec. 2009.

[18] R. Bartinikas, *Electrical Insulating Liquids*. Philadelphia, PA, USA: ASTM, 1994.

BO QI (M'12) received the B.S. degree in electrical engineering and the M.S. and Ph.D. degrees in high voltage and insulation from North China Electric Power University, in 2003, 2006, and 2010, respectively. He is currently an Associate Professor with the School of Electric and Electronic Engineering, North China Electric Power University. His current research interests include electrical insulation and condition monitoring of power apparatus.

CHUNJIA GAO was born in Shandong, China, in August 1991. He received the B.E. degree in electrical engineering from China Agricultural University, in 2013. He is currently pursuing the Ph.D. degree in electrical engineering with the School of Electrical and Electronic Engineering, North China Electric Power University. His current research interests include electric field and space/interface charge characteristics in electrical insulation structures.

HAO HAN was born in Henan, China, in February 1993. He received the B.E. degree in electrical engineering from Beijing Forestry University, in 2015. He is currently pursuing the master's degree in high voltage and insulation technology with the School of Electrical and Electronic Engineering, North China Electric Power University. His current research interests include electric field and space/interface charge characteristics in electrical insulation structures.

XIAOLIN ZHAO was born in Shandong, China, in November 1988. He received the B.S. and Ph.D. degrees in electrical engineering from North China Electric Power University, in 2011 and 2017, respectively. He is currently an Engineer with the China Electric Power Research Institute. His current research interest includes condition monitoring of power apparatus.

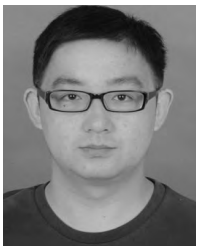

QING YUAN was born in Baoding, China, in 1989. He received the B.S. degree in electrical engineering from North China Electric Power University, in 2013, where he is currently pursuing the Ph.D. degree in electrical engineering. His current research interest includes condition monitoring of power apparatus.

SHUQI ZHANG was born in Liaoning, China, in 1981. He received the bachelor's and M.S. degrees in electrical engineering from North China Electric Power University, Beijing, China, in 2005 and 2007, respectively. In 2007, he joined the China Electric Power Research Institute, where he is a Senior Engineer and the Director of the General Office, Department of High Voltage. He is also currently pursuing the Ph.D. degree with NCEPU. His current research interests are high voltage insulation technologies and transformer related technologies.

CHENGRONG LI (SM'03) was born in Xian, China, in March 1957. He received the B.S. and M.S. degrees in electrical engineering from North China Electric Power University, in 1982 and 1984, respectively, and the Ph.D. degree in electrical engineering from Tsinghua University, in 1989. In 1992, he joined the University of South Carolina, USA, as a Postdoctoral Research Fellow. He joined North China Electric Power University (NCEPU), in 1995, where he is currently a Professor with the Department of Electrical Engineering. His current research interests include gas discharge, electrical insulation and materials, and condition monitoring of power apparatus.